Factors governing the solid phase distribution of Cr, Cu and As in contaminated soil after 40 years of ageing

Stacie Tardif[1*], Sabrina Cipullo[2], Helle U. Sø[3], Joanna Wragg[4], Peter E. Holm[1], Frederic Coulon[2], Kristian K. Brandt[1], Mark Cave[4]

[1]University of Copenhagen, Department of Plant and Environmental Sciences, Frederiksberg, DK-1871, Denmark

[2]Cranfield University, School of Water, Energy and Environment, Cranfield, MK43 0AL, UK

[3]Geological Survey of Denmark and Greenland, Copenhagen K, DK-1350, Denmark

[4]British Geological Survey, Keyworth, Nottingham, NG12 5GG, UK

*Corresponding author: stta@plen.ku.dk

Abstract:

1. The physico-chemical factors affecting the distribution, behavior and speciation of chromium (Cr), copper (Cu) and arsenic (As) was investigated at a former wood impregnation site (Fredensborg, Denmark). Forty soil samples were collected and extracted using a sequential extraction technique known as the Chemometric Identification of Substrates and Element Distributions (CISED) and multivariate statistical tools (redundancy analysis) were applied. CISED data was linked to water-extractable Cr, Cu and As and bioavailable Cu as determined by a whole-cell bacterial bioreporter assay. Results showed that soil pH significantly affected the solid phase distribution of all three elements on site. Additionally, elements competing for binding sites, Ca, Mg and Mn in the case of Cu, and P, in the case of As, played a major role in the distribution of these elements in soil. Element-specific distributions were observed amongst the six identified soil phases including residual pore salts, exchangeable, carbonates (tentative designation), Mn-Al oxide, amorphous Fe oxide, and crystalline Fe oxide. While Cr was strongly bound to non-extractable crystalline Fe oxide in the oxic top soil, Cu and notably, As were associated with readily extractable phases. While water-extractable Cu and As significantly correlated to CISED identified soil phases, water-extractable Cr and bioavailable Cu did not, the latter suggesting that sequential extraction schemes may not be ideally suited for inferring bioavailability and toxicity of elements to ecological endpoints such as microbes in soil. Findings from this study suggest that after 40 years of ageing, Cu and As at CCA-contaminated field sites constitute the highest risk to environmental and human health through ecotoxicological impact and leaching to groundwater reservoirs.

Introduction

Multi-element contaminated sites resulting from anthropogenic activity are of serious concern as: (1) these types of contaminants accumulate and persist in the environment, (2) complex chemical mixtures of elements behave differently from each other in soil and (3) the interactions between elements and potential synergistic effects are not well understood. Chromated copper arsenate (CCA) contaminated sites are a result of the wood impregnation industry which, for several decades, used a solution of salts (CrO_3 and CuO) and arsenic acid (H_3AsO_4) to impregnate wood to preserve it from decay by biotic and abiotic factors (Humphrey, 2002). As environmental legislations in Europe (Directive, 2003) and North America became more stringent over the years,

the use of these impregnation mixtures was severely curtailed and numerous sites were closed down, remaining contaminated to this today (Bhattacharya et al., 2002).

During the fixation of CCA-treated wood a number of different chemical reactions occur and their resulting speciation can have significant effects on leachate toxicity and mobility (Hingston et al., 2001). Namely, reactive and mobile hexavalent Cr is reduced to insoluble Cr(III); however a fraction of Cr(VI) may remain oxidized (Gezer and Cooper, 2016). Arsenic is fixed as chromium arsenates, but As(V) can be reduced to the toxic and mobile As(III) in soil (Nielsen et al., 2010). Chromium, Cu and As, in the form of Cr(VI), Cu(II), and As(III), can cause significant environmental impact, primarily as a result of leaching to groundwater reservoirs and transport to downstream lakes and streams (Nielsen et al., 2013) and due to their high toxicity to soil and water-dwelling organism alike (Gezer and Cooper, 2016; Nunes et al., 2016). Past studies of CCA mixtures have reported that Cu was generally immobilized in the oxic top soil while Cr and As exhibited high spatial mobility and risk of leaching (Allinson et al., 2000; Andersen et al., 1996; Carey et al., 2002; Hopp et al., 2006). However, these studies have been focused on short-term monitoring and/or under controlled laboratory environments and therefore do not provide a useful basis for determining element speciation and mobility in the field after substantial ageing processes (Allinson et al., 2000; Andersen et al., 1996; Carey et al., 2002; Hopp et al., 2006).

Several sequential extraction techniques are available to quantify the distribution of elements in soil phases, providing valuable tools to make assumptions on element speciation and mobility in the field (Bacon and Davidson, 2008). In general, the extractable phases are categorized as exchangeable, specifically adsorbed, carbonates, Fe and Mn-oxides, organic matter and sulphides, and mineral lattice or residual (Cave and Harmon, 1997; Cave and Wragg, 1997). Among sequential extraction methodologies, the Chemometric Identification of Substrates and Element Distributions (CISED) provides an estimate of how much of the potentially harmful elements can be found in each soil solid phase. This approach was developed as a result of limitations/weaknesses associated with ‘classical’ sequential extractions (Cave et al., 2004): lack of specificity for the target phase,

methodological definition of the distribution of elements and re-adsorption of liberated metals, the varied (and sometimes long) extraction times required to undertake the methodology, and the complexity of the extraction matrices for analysis. The CISED methodology considers that a soil and its associated phases are multi-elemental and has taken the approach of using a non-specific acid extractant at increasing strengths combined with mixture resolution analysis to combat the limitations outlined above (Cave et al., 2004). It has been successfully validated by comparison to other sequential extraction procedures such as the Tessier method (Cave and Wragg, 1997), to backscattered scanning electron microscopy (BSEM) analysis and digital energy-dispersive X-ray microanalysis (Cave et al., 2004) and applied to diverse soil samples (Cipullo et al., 2018; Wragg and Cave, 2012; Wragg et al., 2014). Furthermore, although the link between human oral bioaccessibility and CISED has been studied (Cox et al., 2013; Wragg and Cave, 2012; Wragg et al., 2014), the relationship between elements associated with CISED identified solid phases and bioavailable elements, in the context of biological receptors such as bacteria, remains unexplored.

Physico-chemical factors, such as pH (Lu et al., 2005), organic C (Andersen et al., 1996), reactive Fe oxides (Yang et al., 2002) and P content (Bolan et al., 2013; Cao and Ma, 2004), all play an important role in influencing the adsorption and occlusion of these elements between the soil solid and liquid phases. However, studying the complex relationships between physico-chemical factors and element distribution amongst phases in the field can be very challenging and requires the use of multivariate statistical tools. Redundancy analysis (RDA), a form of constrained ordination founded on the principles of multiple linear regression, can test the relationships between multivariate explanatory and response datasets (Legendre and Anderson, 1999) and allows us to explore such complex relationships in the field.

To our knowledge, no field studies investigating the physico-chemical factors governing the solid-phase distribution of CCA in aged soils have occurred. To this end, we collected soil samples along a contamination gradient at a CCA legacy site and assessed the factors affecting the solid-phase distribution of Cr, Cu and As in the field. The study objectives were: (i) to identify the common soil

94 solid phases on site and the distribution of Cr, Cu and As amongst these phases, (ii) to study the
95 influence of different physico-chemical factors on this solid phase distribution, and finally, (iii) to
96 test the relationship between water extractable Cr, Cu and As and bioavailable Cu, as determined by
97 a whole-cell bacterial bioreporter assay, with elements distributed amongst the CISED easily
98 extractable phase.

99

100 ## 2. Materials and Methods

101 ### 2.1. Field site history and geology

102 The multi-element field contaminated site, located in Fredensborg, Denmark (55˚57N, 12 ˚21E),
103 was used as a wood impregnation site, coating wood telephone poles with a mixture of CCA for
104 over 20 years (**Fig. 1a**). The most recent impregnation liquid being used on site was a water soluble
105 formulation of salts CrO_3 (Cr(VI)) and CuO (Cu(II)) and arsenic acid As_2O_5 (As(V)) as 34%, 27%
106 and 25% respectively (Nielsen et al., 2014). The main contamination on site was derived from
107 drippings of surplus preservatives into the soil. In 1976, the entire site was abandoned and left as a
108 brownfield in the surrounding forest. It was replanted in clearly visible rows of birch (*Betula*) and
109 oak (*Quercus*), and today, trees are found in various states of growth because of the heterogeneous
110 soil contamination.

111 In 1989, a full-scale site investigation was launched and reports on the bedrock geology and soil
112 chemistry by the company Samfundsteknik were published (Samfundsteknik, 1989a;
113 Samfundsteknik, 1989b) and an updated site investigation for the period between 1977 and 2009
114 was reported by Nielsen et al. (2010). Briefly, the 1989 investigation reported that soil
115 contamination was widespread across the 65,000 m^2 site as a result of direct spillage and dripping
116 from highly contaminated bark during the drying process. The main contamination on sites derive
117 from the metals Cr (Cr^{3+} and Cr^{6+}), Cu and metalloid As (As^{3+}, As^{5+}), in the top soil and shallow
118 groundwater. Top soil (0-0.5m) was found to be the most heavily contaminated with average

concentrations of 4-700 mg kg $^{-1}$, 6-1500 mg kg^{-1} and 2-1000 mg kg^{-1} for Cr, Cu and As, respectively (**Fig. 1b**: modified from Samfundsteknik report).

The bedrock geology at this site is predominantly a sandy glaciofluvial formation with lenses of sand and clay. The site is located on the edge of the regional formation of the Alnarp Valley, which extends across Northern Zealand and South of Sweden. The contaminated site is found upstream of the Esrum Lake and connected via shallow, intermediate and deep aquifers, with local sediments constituting one of the most important groundwater reservoirs in North Zealand, Denmark. Nielsen et al. postulated that the most likely route for CCA leaching to the lake being the intermediary and deep aquifers (Nielsen et al., 2010).

2.2. Experimental design and soil sampling

Ten sampling stations (1-10) were established at this site in October 2016. The sample selection was based on the 1989 site investigation concentrations and a preliminary sampling (data not shown) validating the establishment of a contamination gradient (**Fig. 1b**). At each location a plot of 1 m^2 was laid out and each plot separated into 4 quadrants with the intention of sampling biological replicates. It became apparent after soil chemical analysis, however, that heterogeneity on site was extensive and as a result, samples were kept separate for downstream analysis. Samples were named from 1-40 based on total cumulative Cr, Cu and As concentrations in the samples.

Approximately 500 g of top soil (~10 cm in depth) was collected from each quadrant in a randomized sampling design within the quadrant and mixed thoroughly on site in plastic bags in order to obtain a representative sample (10 sampling locations × 4 quadrants = 40 samples). Individual fresh soil samples were divided and processed for analysis in the following way (**Supplementary Fig.1**): (1) 2 g into 15mL falcon tube for water-extraction/bacterial bioreporter; (2) 5 g into 50mL falcon tube for pH measurement; (3) 10 g in petri-dish for water content measurement; (4) 5 g in airtight anoxic vials and stored at -20 °C for reactive Fe oxide measurement and (5) 10 g was pooled from each quadrant into one composite sample for each sampling location

and thoroughly homogenized for texture analysis. Remaining soil was air-dried, sieved (2 mm mesh size) and ground to a fine powder with mechanical pestle and mortar (henceforth referred to as pulverized) for downstream physical-chemical analyses (Supplementary F1).

2.3. Soil physico-chemical analyses

Particle size distribution was determined on composite fresh soil by the hydrometer method (Gee and Bauder, 1986) and classified according to international standard particle size classes. Water content was measured after drying samples for 12h at 105˚C. Soil pH was measured on fresh soil in MilliQ water at a 1:2.5 ratio (soil liquid, w/v) using a combined glass electrode (Metrohm, 6.0228.000). Poorly crystalline Fe oxides, henceforth referred to as reactive fraction of Fe oxides, were measured based on the experimental procedures described in Nguyen et al. (2014). Two chemical extractions were performed in parallel for 24 hours in 1:100 (soil liquid, w/v) using: 1) 0.5M formic acid at pH 3, targeting the carbonates and phosphates and 10mM ascorbic acid and 2) 0.5M formic acid at pH 3, to target the ferrihydrite and very poorly crystalline goethite. Poorly crystalline Fe oxides was determined by subtracting Fe^{2+} found in the first extraction from Fe^{2+} in the second extraction. Total carbon and total nitrogen concentrations were analyzed by dry combustion at 1200° using a Vario Macro cube C/N elemental analyzer on dry, 2mm sieved and pulverized soil samples (Elementar Analysen systeme GmbH, Hanau, Germany). Data quality of C/N analysis was evaluated by inclusion of standard reference materials (1515 Apple leaves and 141d acetanilide, National Institute of Standards and Technology (NIST), Gaithers-burg, MD, USA). Plant-available P was determined by the Olsen P method, extracting the dry, 2mm sieved and pulverized soil with a 0.5M hydrogen carbonate solution at pH 8.5 and then spectrophotometrically measuring the P content in solution, following ISO 11263:1994 protocol.

2.4. Water-extractable, total and CISED extractions

167 Water-extractable elements (Al, As, Ba, Ca, Cd, Co, Cr, Cu, Fe, K, Li, Mg, Mo, Mn, Na, Ni, P, Pb,
168 S, Sb, Si, Se, Sr, V and Zn) were analyzed in soil-water extracts at a 1:5 ratio (soil liquid, w/v),
169 extracted on a horizontal shaker at 200rpm for 2 hours.

170 Total element concentrations (Al , As, Ba, Ca, Cd, Co, Cr, Cu, Fe, K, Li, Mg, Mo, Mn, Na, Ni, P,
171 Pb, S, Sb, Si, Se, Sr, V and Zn) were determined following ISO 11047 protocol, which extracts the
172 elements with aqua regia (HCl/HNO_3) using a microwave digestion system.

173 The solid phase distribution of elements (Al , As, Ba, Ca, Cd, Co, Cr, Cu, Fe, K, Li, Mg, Mo, Mn,
174 Na, Ni, P, Pb, S, Sb, Si, Se, Sr, V and Zn) was investigated using a modified non-specific sequential
175 extraction method, based on the CISED methodology (Cave et al., 2004), as described in (Cipullo et
176 al., 2018). Briefly, 2 g of pulverized soil was sequentially extracted (twice per reagent) with
177 deionized water (DI) and HNO_3 in increasing dissolution strength: DI (E1-E2), 0.01 M (E3-E4),
178 0.05 M (E5-E6), 0.1 M (E7-E8), 0.5 M (E9-E10), 1.0 M (E11-E12) and 5.0 M (E13-E14), with
179 H_2O_2 (100 Volumes) addition in the last 4 extracts.

180 **2.5. Bacterial bioreporter assay**

181 Henceforth, Bioavailable Cu (Cu_{bio}) is operationally defined as Cu species in soil-water extracts that
182 are able to induce gene expression in a Cu-specific *Pseudomonas fluorescens* bioreporter during a
183 90 minute incubation period. A dual strain whole-cell bacterial bioreporter assay was performed
184 using the same soil-water extracts as above, as described previously (Brandt et al., 2008). No
185 sample matrix correction factors were required.

186 **2.6. Element measurement by Inductively Couple Plasma-Mass Spectrometry**

187 Water-extractable, aqua regia and CISED samples were diluted (1:10) with HNO_3, spiked with 5 µg
188 mL^{-1} of internal standard mix (Se, Ge, Rh, and Bi), and subsequently measured for elements listed
189 above using an Inductively Couple Plasma-Mass Spectrometry (NexION® 350D ICP-MS, Perkin
190 Elmer). The instrument was calibrated with 9 major (Ca, Fe, K, Mg, Mn, Na, S, Si, P) and 17 trace

(Al, As, Ba, Cd, Co, Cr, Cu, Hg, Li, Mo, Ni, Pb, Sb, Se, Sr, V, Zn) elements. The concentration ranged from 1 to 40 mg L^{-1} for major elements and 0.01 to 2 mg L^{-1} for trace elements. For data quality control, acid blanks (1% nitric acid), digestion blank, and guidance material (BGS102) were analyzed systematically, to account for blank contamination, sensitivity, operating conditions and extraction accuracy. No recovery corrections were made as the mean repeatability (expressed as relative standard deviation %) of the guidance material (BGS102) was below 15% for individual elements. Sample 8 was removed from subsequent data analyses, as it did not meet the data quality control criteria.

2.7. CISED self-modelling mixture resolution

The self-modelling mixture resolution (SMMR) algorithm (MatLab Version R2015a) was used to model the solid-phase distribution of elements in soil as studied by the CISED sequential extraction technique (Cave et al., 2004). The algorithm assumes that the chemical analysis data represents different proportions of chemical components (which have fixed chemical composition) that have been dissolved out of the soil by the extraction media. The algorithm then uses chemometric methods to identify the number of components being extracted, the chemical composition (Al, As, Ba, Ca, Cd, Co, Cr, Cu, Fe, K, Li, Mg, Mo, Mn, Na, Ni, P, Pb, S, Sb, Si, Se, Sr, V and Zn) of each component (CMP = composition) and the amount of each component in each extraction solution. The extraction profile of each component is derived from the amount of each component found in the 14 extracts (PRF = profile). In addition, the relative proportions of each element in each component can also be calculated (DST = distribution). The SMMR algorithm was run separately for each sampling location, including the 4 quadrants, resulting in 10 distinct sets of components (6-13/sampling location), resulting in a total 89 individual components in the entire dataset. From here, hierarchal clustering, geochemical profile interpretations and previous study with a certified reference material (Cave et al., 2004; Wragg and Cave, 2012) was used to classify the 89 components into the common, distinct soil phases (i.e. residual pore salts, exchangeable phases,

etc.).. Briefly, a matrix with mean-centered and scaled CMP and PRF, as described above, of each component was performed with Ward's method using the 'agnes' function in the cluster package (Maechler et al., 2012) in R (v.3.4.1, R Foundation for Statistical Computing; available at https://www.r-project.org/. The result from the clustering was visualized using a heatmap (**Fig. 2**) created using ggplot2, reshape2, grid, and ggdendro packages (Wickham, 2007; Wickham, 2010).

2.8. Statistical analyses

All statistical analyses were performed in R (v.3.4.1, R Foundation for Statistical Computing). The significant influence of specific physico-chemical soil parameters on the solid phase distribution of Cr, Cu and As was tested using redundancy analyses (RDA) (Legendre and Anderson, 1999). In the context of this research, it tested the relationship between physico-chemical properties of soil on the solid phase distribution of either Cr, Cu or As (separate analysis for each element). In order to choose which explanatory variables (physico-chemical factors) to include in the model, we pre-selected physico-chemical parameters based on geological interpretation of the system, keeping in mind that one of the central assumptions of this analysis is independence between explanatory variables. Variables selected for hypothesis testing were based on evidence from the literature and included pH, total C, reactive Fe oxide, Olsen P, total P as well as total and water-extractable Ca, Mg and Mn. A forward selection of variables using the 'ordistep' function in the 'vegan' package was performed in order to select the variables to include in the final model. The final model was built using the 'rda' and 'anova.cca' functions of the 'vegan' package (Oksanen et al., 2013). Spatial autocorrelation between samples due to sampling design tested positive using the 'mso' function in the 'vegan' package. Thus, it was accounted for using partial redundancy analysis, conditioning for sampling location. Reported adjusted redundancy statistics R^2 were obtained using the 'RsquareAdj' function of the 'vegan' package.

The relationship between elements in the water-extracts, bioavailable Cu and the common CISED identified soil phases was not reported as it is generally assumed that soil particle associated-

241 elements are not directly available to bacteria (Brandt et al., 2006; Noll, 2003). Therefore, we tested
242 the relationships between bioavailable Cu (ug g^{-1}), water-extractable Cr, Cu and As (ug g^{-1}) and
243 elements (ug g^{-1}) in the most easily extractable soil component identified by CISED for each
244 sampling location by using Pearson correlation coefficient with the 'cor' function in R.

245

246 ## 3. Results

247 ### 3.1 Soil physico-chemical properties

248 Selected physico-chemical soil properties are summarized in **Table 1** and detailed characterization
249 is provided in **Supplementary Table 1** and **Table 2**. Total concentrations of Cr, Cu and As ranged
250 between 26.1-1819 mg kg^{-1}, 17.2-2205 mg kg^{-1} and 32.4-2839 mg kg^{-1}, respectively, while water-
251 extractable concentrations ranged from 0.02-0.78 mg Cr kg^{-1}, 0.11-5.99 mg Cu kg^{-1} and 0.17-18.3
252 mg As kg^{-1} and bioavailable Cu ranged from 0.04-3.52 mg kg^{-1}.

253 Soil samples collected from location 1, 2, 3, 5, 6 and 8 were classified as sandy soils (sand >
254 85.0%) while 4, 7, 9 and 10 were loamy sand (sand = 81.0- 85.0 %). pH ranged from 3.53-6.83
255 across all samples. Total C, ranged from 1.47-17.4% and total N from 0.09-0.83%. Reactive Fe
256 oxides in samples ranged from 1.48-5.97 mg kg^{-1}, Olsen P 14.7-73.4 mg kg^{-1} and total P 319-713 μg
257 g^{-1}. Total and water-extractable Ca ranged from 1112-7414 μg g^{-1} and 3.42-50.8 μg g^{-1}, respectively.
258 Total and water-extractable Mg ranged from 692-1951 μg g^{-1} and 0.66-6.72 μg g^{-1}, respectively.
259 Total and water-extractable Mn ranged from 225.4-1174 μg g^{-1} and 0.08-2.45 μg g^{-1}, respectively.

260 ### 3.2 Soil solid phases identified by CISED

261 Extraction recoveries with the CISED extraction methodology compared with total element
262 concentration averaged 61 ± 13 %, 90 ±11% and 81 ± 11% for Cr, Cu and As, respectively. The
263 cumulative CISED extraction recoveries were less than 100 % because the CISED extraction
264 protocol mainly targets the easily soluble surface coatings and not the silicate matrix of soil.

265 The SMMR algorithm identified 6-13 soil components per sampling location giving 89 individual
266 components in the entire dataset. Using a combination of the chemical composition of the clusters,
267 the relative ease of their extraction as indicated by the amount extracted at each step and a general
268 knowledge of soil geochemistry, 6 common physico-chemical phases were identified **(Fig. 2**).
269 **Table 2** describes the 6 common soil solid phases amongst the sampling locations, listed here in
270 decreasing ease of extractability: Residual pore salts, exchangeable, carbonates (tentative
271 designation), Mn-Al oxide, Fe oxide (amorphous) and Fe oxide (crystalline) (**Table 2**).

272 *Residual pore salts*-this cluster was extracted primarily during the first two extractions of CISED
273 using deionized water. It is dominated by Ca, Na, K, and Si, which are highly mobile elements and
274 can be derived from soluble pore water salts in soil.

275 *Exchangeable*-this cluster does not result in defined peaks like the other phases, likely as a result of
276 data processing of soil components of higher variability, and is comprised of several components
277 from each location. It is mainly comprised of exchangeable cations such as Na, Mg, S, Sb, Se and P,
278 which are typically bound to soil particle surfaces by weak electrostatic forces and can be displaced
279 by competing cations and released into solution, as exhibited in the saw toothed pattern of the
280 extraction profile (**Table 2**). Some of these extractable components also come out at higher acid
281 strengths, conceivably being encased in more recalcitrant components which are only being released
282 later on in the extraction profile.

283 *Carbonates (tentative designation)*- typically we would designate this component as carbonates
284 however, due to the inherent physico-chemical properties (pH below 7) on site, which would
285 suggest that carbonates are unlikely to occur, we only tentatively assign this soil phase. This is
286 further discussed in Supplementary Material. This cluster is extracted on the first addition of acids
287 and is comprised of two sub-clusters which are carbonate (Ca-Mg) and carbonate (Ca). Carbonate
288 (Ca-Mg) sub-cluster is dominated with Ca and Mg, and comes out over a narrow range in the
289 extractions, primarily during the addition of 0.01M nitric acid. Other elements present in this

290 partition include Al, Ba, Cd, Cu, Sr and Zn. Carbonate (Ca) sub-cluster comes out a little later in the
291 extraction profile, indicating that this carbonate phase is less available than the previous. It is
292 composed of the same elements as the previous cluster, with the notable absence of Mg. Location 3,
293 4, 5, 8 and 10 have soil components in both sub-clusters while Location 1, 2, 6, 7 and 9 only have
294 soil components associated with more readily available carbonate phase (Ca-Mg).

295 *Mn-Al oxide*- this cluster is dominated by Mn and Al elements and tends to be extracted upon
296 addition of peroxide, a reagent commonly known to target Al oxides.

297 Two distinct clusters of Fe oxides were identified and suggest the presence of both amorphous and
298 crystalline Fe oxides:
299 *Fe oxide (amorphous)*- this cluster comprises soil components that are extracted from 0.1M-1M nitric
300 acid and are primarily made up of Fe and to a lesser extent, Al, Pb, Se and V.
301 *Fe oxide (crystalline)*- this cluster is comprised primarily of Fe and to a lesser degree Al and Si, and
302 requires high acid concentrations (0.5-5M) to extract. Within this cluster, there is a subcluster with
303 3 soil components belonging to the locations with the highest contamination (Location 3, 4 and 5)
304 and appear to be a CCA component, primarily made up of Fe, Cr and As.

305 **3.3 Solid Phase Distribution of Cr, Cu and As in soil**

306 Chromium, Cu and As at this site were associated with specific soil phases along the contamination
307 gradient. **Fig. 3** presents the data based on percentage of the individual element in the soil phases as
308 compared with the total Cr, Cu, As extracted in that sample with CISED and as such, the changes
309 observed are relative. The distribution of Cr, Cu and As (μg g^{-1}) in each soil phase can be found in
310 **Supplementary Table 3**. Samples were separated into low, moderate and high contamination the
311 subsequent text in order to discuss their distribution along the contamination gradient, as follows:
312 (i) Low concentrations, samples 1-14 (below 175 μg g^{-1} for Cr, Cu and As), (ii) moderate
313 concentrations, samples 15-27 (between 175-200 for Cr, 175-600 for Cu and 175-400 μg g^{-1} for

As), and (iii) high concentrations, samples 28-40 (above 200 for Cr, 600 for Cu and 400 μg g^{-1} for As).

Cr is almost exclusively found in the least reactive phase, in the crystalline Fe oxide. In the low contamination, particularly in samples coming from location 9, Cr is present in the exchangeable (avg. 78± 11 %) and Mn-Al oxide (avg. 22±11 %) phases. In the high contamination, at location 3, some Cr is found in the exchangeable phase (avg. 42±10 %). In the low and moderate contamination, some Cr is found in the amorphous Fe oxide phase (avg. 18 ±8 %) at location 8 and 2.

Cu is primarily found in Mn-Al oxides and to a lesser extent, the Fe oxide (amorphous) phases in the lower end of the contamination gradient. In the moderate and high contamination, Cu is almost exclusively found in the carbonate (tentative designation) phase (avg. 57±29 %). It is primarily found in the less extractable carbonate sub-cluster, carbonate (Ca). At location 9 (avg. 33±25 %) as well as locations 3 (avg. 17±8 %) and 4 (avg. 18±6 %), a portion of the Cu is found in the exchangeable phase.

The As solid phase distribution pattern along the contamination gradient was more variable. At low contamination, it was primarily in the crystalline Fe oxides (avg. 46±21 %), in the Mn-Al oxides (avg. 10 ±8 %), and amorphous Fe oxides (avg. 16 ±6 %). For samples from location 9, it is also in the exchangeable phase (avg. 24 ±23 %). In the moderate contamination, the As contamination shifts into the exchangeable (avg. 18±13 %), Mn-Al oxides (avg. 18 ±13 %) and amorphous Fe oxides (avg. 34±22 %). In the high contamination, the As was no longer found in the Mn-Al oxides but in the carbonates (tentative designation) (avg. 22±7 %), amorphous Fe oxides (avg. 18 ±10 %), crystalline Fe oxides (avg. 33±11 %) and also in the exchangeable (avg. 24±3 %) for locations 3 and 4. In the moderate (avg. 4±3 μg g^{-1}) and high contamination (avg. 2±1 %), a small proportion of As could be detected in the residual pore salts, corresponding to alarmingly high concentrations in specific samples (up to 37.5 μg g^{-1}).

3. 4 Factors affecting the Solid-Phase Partitioning of Cr, Cu and As in Soil

Specific physico-chemical parameters significantly affected the solid-phase partitioning of Cr, Cu and As in soil as shown with partial redundancy analyses (**Fig. 4**). Cr solid phase distribution was significantly affected by pH (F=10.3, p=0.002), with the model adjusted R^2=0.194 (**Fig. 4a**). The amount of variance explained by this model was 20.9% and an additional 6.1% of the variation could be attributed to spatial autocorrelation correction. Cu solid phase distribution was significantly affected by total Mg (F=29.1, p=0.001), Olsen P (F=24.9, p=0.001), pH (F=22.4, p=0.001), total Mn (F=14.0, p=0.003), water-extractable Mg (F=13.3, p=0.001) and water-extractable Ca (F=6.2, p=0.018), with the model adjusted R^2=0.759 (**Fig. 4b**). The amount of variance explained by this model was 70.0% and an additional 8.1% of the variation could be attributed to spatial autocorrelation correction. As solid phase distribution was significantly affected by pH (F=24.3, p=0.001), reactive Fe oxides (F=5.2, p=0.022) and Olsen P (F=3.4, p=0.05), with the model adjusted R^2=0.437 (**Fig. 4c**). The amount of variance explained by this model was 46.5% and an additional 9.0% of the variation could be attributed to spatial autocorrelation correction.

3. 5 Linking Cr, Cu and As solid phases to bioavailability

While water-extractable Cu (r=0.374, p=0.019) and As (r=0.612, p<0.001) were significantly correlated to the most readily available CISED component at each site, water-extractable Cr and bioavailable Cu were not.

4. Discussion

To our knowledge, this is the first study to investigate and elucidate specific effects of physico-chemical parameters on the solid phase distribution of elements at a complex field site after substantial ageing processes. Element-specific distributions and behaviors in soil were observed along a CCA-contamination gradient at former wood impregnation site.

4.1 Factors affecting the Solid-Phase Partitioning of Cr, Cu and As in Soil

Although past studies have already demonstrated that pH can alter the distribution of these individual elements in soil (Kabata-Pendias, 2010; Lu et al., 2005), here we report the importance of pH in affecting the distribution of all three elements simultaneously along a field contamination gradient. These finding suggest that acidification of soil, as a result of events such as rainwater leaching, decomposition of organic matter and release of carbon dioxide and/or plant root exudation of reducing and chelating compounds for example, could lead to redistribution of Cr, Cu and As amongst soil solid phases.

Additionally, element-specific influences were observed. Cu distribution was influenced by divalent cations such as Ca^{2+}, Mg^{2+} and Mn^{2+}, which are known to be structurally similar and may compete with Cu for binding sites in soil. For example, competition for binding sites and translocation into plant roots between divalent cations such as Ca and Mn has been reported with Cd (Eller and Brix, 2016). Plant available P (Olsen P) was also shown to be important in influencing the distribution of Cu, and could compete with Cu for binding to different oxides, such as Mn-Al oxides. In the case of As, reactive Fe oxides were significantly affecting its distribution, a phenomenon generally known (Yang, Barnett et al. 2002). Available P (Olsen P) also played a role in the distribution of As on soil solid phases. Interestingly, As(V) is a well-known phosphate analog which competes for sorption sites in soil (Bolan et al., 2013). Thus, an increase in P could result in an increase in available As for plant uptake, as demonstrated at a CCA site by Cao et al. (2004). Indeed, this suggests that sudden changes in these specific physico-chemical factors could lead to shifts in the distribution of these elements between soil liquid and solid phases, as discussed in the subsequent section 4.2.

4.2 Solid Phase Distribution of Cr, Cu and As in soil

In the wood impregnation mixture, Cr was found as Cr(VI), a highly reactive, mobile and toxic form of Cr. During the fixation process, it is reduced to Cr(III) but residues of Cr(VI) may still occur and leach into the soil. After a substantial ageing period, Cr on site was found almost

388 exclusively bound to the least extractable phase, the crystalline Fe oxide. Although the crystalline
389 Fe oxide minerals typically have lower adsorption capacity than amorphous phases such as
390 ferrihydrite minerals, the dominance of Cr in the aforementioned phase could be for several reasons.
391 Either there are more of these oxides present at this site and therefore a larger fraction is absorbed
392 onto this fraction, and/or perhaps more importantly, ferrihydrites age to crystalline Fe oxide over
393 time, a process which can be further aided by microbes in soil (Zachara et al., 2002) and as such, Cr
394 may have started off associated with ferrihydrites but this fraction became crystalline over time. As
395 a result, and in line with a previous report at this site (Nielsen et al., 2016), we suggest that the
396 dominant form of Cr in the top soil is Cr (III) because in this form, Cr is typically bound to
397 positively charged surfaces such as Fe and Al oxides and is very stable in soil (Namiesnik and
398 Rabajczyk, 2012). Although past laboratory and field studies have suggested that Cr from the CCA
399 mixtures is highly mobile, these studies have focused on short-term monitoring (Allinson et al.,
400 2000; Hopp et al., 2006). After 100 days of ageing, however, Carey et al. demonstrated in a
401 controlled leaching study, that less than 1% of Cr(VI) could be extracted in the top layer (Carey et
402 al., 2002) . Groundwater investigations of the terrain magazines at this site have suggested that the
403 mobile pools of Cr have been washed out, as concentrations in the groundwater have fallen
404 significantly between 1977 and 1995, from 21-1500 μg L^{-1} to <3 μg L^{-1} (Nielsen et al., 2010).
405 Remaining Cr(VI) in the top soil was likely reduced to chromic cation Cr(III) by soil organic
406 matter, as previously shown (Carey et al., 2002; Kabata-Pendias, 2010). Although total
407 concentrations of Cr at the higher end of the contamination gradient exceed guideline values, it is
408 unlikely to leach and cause adverse ecological impact because of its association with crystalline Fe
409 oxide structures which are stable under oxic top soil conditions.

410 Cu, added as CuO salts in the impregnation mixture, is typically found as a divalent cation in soil.
411 After 40 years of ageing, Cu(II) occurred in readily available phases such as exchangeable, and less
412 available phases such as carbonates (tentative designation) and Mn-Al oxides. Previously, Cu(II) in
413 the oxic top soil has been shown to be highly reactive with soil organic matter (SOM), typically

414 exhibiting low mobility in soil (Andersen et al., 1996; Kabata-Pendias, 2010). At this site, however,
415 soil organic matter content is generally low (avg. 5.6±4.2%), particularly in the highly contaminated
416 end of the gradient where substantial amounts of Cu are bound (avg. 2.0±0.5%), suggesting that Cu
417 might not efficiently bind to SOM. In recent work at this contaminated site, Frick et al. (*submitted*)
418 also found that dissolved organic matter content in soil from the highly contaminated samples was
419 very low. Indeed, in their artificially CCA contaminated soils with low organic content, Balasoiu et
420 al., found that Cu was predominantly bound to soluble or exchangeable soil phases (Balasoiu et al.,
421 2001). In samples from the low contamination gradient at this site, Cu binds readily to Mn-Al oxides
422 and amorphous Fe oxide, which has been demonstrated in several soils with low organic matter soils
423 (Agbenin and Olojo, 2004; Yu et al., 2004). When moving towards the moderate to highly
424 contaminated samples, Cu shifted into the more extractable phase, carbonates (tentative designation)
425 (primarily the less extractable carbonate sub-cluster). Indeed, the differential vegetation cover and,
426 changes in plant species and physiology between the sampling location on site will affect the
427 geochemistry through direct (e.g. input and quality of organic matter, oxygen content and water
428 holding capacity) and indirect effects on the soil fauna by processes such as reduced organic material
429 breakdown by microorganisms and/or increased compaction of soil due to reduced earthworm activity
430 (Arthur et al., 2012). The absence of trees, as seen in the higher end of the contamination gradient
431 which can only support the growth of mosses, can lead to increased mobility of elements via absence
432 of interception of incident precipitation, root accumulation and precipitation of elements in the
433 rhizosphere and could in part explain the shift of Cu into a more extractable phase. Determining the
434 isolated impact of individual effects discussed above on the solid phase distribution of elements,
435 however, is nearly impossible as these processes add-up and merge to form what is called the legacy
436 effect. Although carbonate associated elements are generally considered non-available to plants, a
437 drop in pH could release Cu to more readily-extractable phases (Martınez and Motto, 2000). In the
438 highly contaminated samples, Cu was also associated to the exchangeable phase at specific locations,
439 a phase which has been described as readily available to plants and microorganisms (Maderova et al.,

2011). Furthermore, the cation characteristics of this phase (e.g. Na, Mg and S), are bound to soil particle surfaces by weak electrostatic forces and can be displaced by competing cations (Rowell, 1994). Indeed, this study has reported that competing divalent cations such as Ca^{2+}, Mg^{2+} and Mn^{2+} play a significant role in the distribution of Cu and as such, the divalent cations in this phase could compete for binding with Cu, leading to the release of Cu in the soil solution. In this study we report that Cu, particularly in highly contaminated samples, is present in soil phases that are readily extractable and/or in phases that are could replenish exchangeable and soil pore water element concentrations, under altering physico-chemical conditions (Degryse et al., 2009).

Arsenic was added as arsenate (As(V)) in the impregnation mixture, which is the less mobile and toxic inorganic form of As as compared with arsenite (As(III)) (Masscheleyn et al., 1991). At this CCA site (Frick et al., *submitted*) and in other studies (Balasoiu et al., 2001; Gräfe et al., 2008; Hopp et al., 2008), As(V) is reported as the dominant form of As, which is consistent with our knowledge that As (V) dominates in oxic top soil environments (Kabata-Pendias, 2010). Along our contamination gradient, we observed that As was associated with all soil solid phases identified with the CISED methodology. A large portion of the As on site was associated with Mn-Al and Fe oxides, in line with our knowledge that the inorganic oxyanion As(V) strongly binds to positively charged Fe and Al oxides, both in natural (Lin and Puls, 2000; Wragg et al., 2014) and contaminated soils (Bhattacharya et al., 2002). Arsenic bound in these phases is least likely to be dissolved in the soil solution and leach to groundwater aquifers. But, As is also associated with readily extractable phases such as residual pore salts and exchangeable. Arsenic concentrations in those phases, reported at up to 37 and 437 μg g^{-1}, respectively, are particularly alarming, given that the soil guidelines for ecological risk are set at 20 μg g^{-1}. Like Cu, As is also found in the carbonates (tentative designation) phase and changes in specific physico-chemical factors such as pH, reactive Fe oxides or available P, as described in section 4.1, could lead to redistribution of As into different soil phases and thus, increase the risk of leaching and contamination of groundwater reservoirs.

4.3 Linking Cu and As in solid phases to bioavailability

There is consensus in the literature that insignificant fractions of soil particle associated-Cu are directly available to bacteria (Brandt et al., 2006; Noll, 2003; Ore et al., 2010). As a result, soil pore water elements are often used to represent the biologically relevant element fraction (Giller et al., 2009; Peijnenburg et al., 2007). This study found that although water-extractable Cu correlated to Cu in the most extractable CISED component, bioavailable Cu measured with a bacterial bioreporter, did not. This is in line with knowledge that bioavailability of Cu is influenced by complexation with dissolved organic matter (Brandt et al., 2008; Nybroe et al., 2008). Results from sequential extraction schemes have been used in the past to make inferences about bioavailability and toxicity to soil dwelling organisms such as plants, invertebrates and microorganisms. Our study has shown, however, that bioavailability of Cu to microorganisms cannot be fully inferred using sequential extraction methodologies such as CISED. Indeed, Maderova et al. (2011) also concluded that no single chemical method, including the BCR sequential extraction methodology they employed in their study, could quantify bioavailability of Cu to microbes. This suggests that it is imperative to have receptor-targeted tests of bioavailability and highlights the importance of including these tests alongside chemical methods.

Water-extractable As was also significantly correlated with As in the most extractable CISED phase, and interestingly, past research at this site reported that water-extractable As was almost exclusively bioavailable, as measured with an arsenic bioreporter assay (Frick, 2016). Collectively these findings suggest that while no inferences can be made about Cu bioavailability from Cu in the CISED residual pore salt phase, As bioavailability to bacteria could tentatively be inferred at this contaminated site.

5. Conclusion/Summary

In this study we demonstrated that physico-chemical factors governing the solid phase distribution of Cr, Cu and As at a CCA-contaminated site are element-specific. Hence, pH and elements competing for binding sites, P in the case of As and divalent cations Ca, Mg and Mn for Cu, affected this distribution. Changes in specific physico-chemical factors through natural processes such as soil acidification from rainwater leaching, organic matter degradation and/or plant exudation or targeted remediation approaches which increase available P or reactive Fe oxides in the field, could alter the solid phase distribution and therefore, mobility of Cr, Cu and As. After substantial ageing processes, Cu and particularly, As remained in readily extractable phases such as residual pore salts and exchangeable while Cr was largely bound to the least extractable solid phase, crystalline Fe oxides. Findings from this study suggest that Cu and As at aged CCA-contaminated sites constitute the largest risks for environmental and human health and should be closely monitored. In the case of Cu, risk is mainly related to ecotoxicological impact while As, due to its higher mobility and severe human health effects, may represent a risk to adjacent aquatic ecosystems and to human health via contamination of drinking water reservoirs. In addition, Cu bioavailability to microbes could not be predicted solely using a sequential extraction procedure. This suggests that receptor-specific tests of bioavailability such as whole cell bacterial bioreporters for microbes are needed to infer bioavailability in the soil environment and should be integrated into risk assessments to complement analytical methods.

Acknowledgements/Funding

This work was supported financially by REMEDIATE (Improved decision-making in contaminated land site investigation and risk assessment) Marie-Curie Innovation Training Network from the European Union's Horizon 2020 Program (grant agreement n. 643087). In addition, we acknowledge the support of the Natural Sciences and Engineering Research Council of Canada (NSERC), [PGS D 396155934]. Cette recherche a été financée par le Conseil de recherches en

515 sciences naturelles et en génie du Canada (CRSNG), [PGS D 396155934]. The author's would like
516 to thank the Danish Soil Partnership for facilitating access to the contaminated site.

517

518 **Conflict of Interests**

519 The authors declare no conflicts of interests

520

521 **References**

522 Agbenin J, Olojo L. Competitive adsorption of copper and zinc by a Bt horizon of a savanna Alfisol
523 as affected by pH and selective removal of hydrous oxides and organic matter. Geoderma
524 2004; 119: 85-95.
525 Allinson G, Turoczy N, Kelsall Y, Allinson M, Stagnitti F, Lloyd□Smith J, et al. Mobility of the
526 constituents of chromated copper arsenate in a shallow sandy soil. New Zealand Journal of
527 Agricultural Research 2000; 43: 149-156.
528 Andersen S, Rasmussen G, Snilsberg P, Amundsen C, Westby T. Assessing toxicity and
529 mobilisation of impregnation salts at a contaminated site. Fresenius' journal of analytical
530 chemistry 1996; 354: 676-680.
531 Arthur E, Moldrup P, Holmstrup M, Schjønning P, Winding A, Mayer P, et al. Soil microbial and
532 physical properties and their relations along a steep copper gradient. Agriculture,
533 ecosystems & environment 2012; 159: 9-18.
534 Bacon JR, Davidson CM. Is there a future for sequential chemical extraction? Analyst 2008; 133:
535 25-46.
536 Balasoiu CF, Zagury GJ, Deschenes L. Partitioning and speciation of chromium, copper, and
537 arsenic in CCA-contaminated soils: influence of soil composition. Science of the Total
538 Environment 2001; 280: 239-255.
539 Bhattacharya P, Frisbie S, Smith E, Naidu R, Jacks G, Sarkar B. Arsenic in the environment: a
540 global perspective. Handbook of heavy metals in the environment. Marcell Dekker Inc.,
541 New York 2002: 147-215.
542 Bolan N, Mahimairaja S, Kunhikrishnan A, Choppala G. Phosphorus–arsenic interactions in
543 variable-charge soils in relation to arsenic mobility and bioavailability. Science of the Total
544 Environment 2013; 463: 1154-1162.
545 Brandt KK, Holm PE, Nybroe O. Bioavailability and toxicity of soil particle□associated copper as
546 determined by two bioluminescent Pseudomonas fluorescens biosensor strains.
547 Environmental Toxicology and Chemistry: An International Journal 2006; 25: 1738-1741.
548 Brandt KK, Holm PE, Nybroe O. Evidence for Bioavailable Copper− Dissolved Organic Matter
549 Complexes and Transiently Increased Copper Bioavailability in Manure-Amended Soils as
550 Determined by Bioluminescent Bacterial Biosensors. Environmental science & technology
551 2008; 42: 3102-3108.
552 Cao X, Ma LQ. Effects of compost and phosphate on plant arsenic accumulation from soils near
553 pressure-treated wood. Environmental Pollution 2004; 132: 435-442.
554 Carey P, Bidwell V, McLaren R. Chromium (VI) leaching from large undisturbed soil lysimeters
555 following application of a simulated copper-chromium-arsenic (CCA) timber preservative.
556 Soil Research 2002; 40: 351-365.

557 Cave MR, Harmon K. Determination of trace metal distributions in the iron oxide phases of red bed
558 sandstones by chemometric analysis of whole rock and selective leachate data. Analyst
559 1997; 122: 501-512.
560 Cave MR, Milodowski AE, Friel EN. Evaluation of a method for identification of host physico-
561 chemical phases for trace metals and measurement of their solid-phase partitioning in soil
562 samples by nitric acid extraction and chemometric mixture resolution. Geochemistry:
563 Exploration, environment, analysis 2004; 4: 71-86.
564 Cave MR, Wragg J. Measurement of trace element distributions in soils and sediments using
565 sequential leach data and a non-specific extraction system with chemometric data
566 processing. Analyst 1997; 122: 1211-1221.
567 Cipullo S, Snapir B, Tardif S, Campo P, Prpich G, Coulon F. Insights into mixed contaminants
568 interactions and its implication for heavy metals and metalloids mobility, bioavailability and
569 risk assessment. Science of The Total Environment 2018; 645: 662-673.
570 Cornell R, Schindler P. Photochemical dissolution of goethite in acid/oxalate solution. Clays Clay
571 Miner 1987; 35: 347-352.
572 Cornell RM, Schwertmann U. The iron oxides: structure, properties, reactions, occurrences and
573 uses: John Wiley & Sons, 2003.
574 Cox SF, Chelliah MC, McKinley JM, Palmer S, Ofterdinger U, Young ME, et al. The importance of
575 solid-phase distribution on the oral bioaccessibility of Ni and Cr in soils overlying
576 Palaeogene basalt lavas, Northern Ireland. Environmental geochemistry and health 2013; 35:
577 553-567.
578 Degryse F, Smolders E, Parker D. Partitioning of metals (Cd, Co, Cu, Ni, Pb, Zn) in soils: concepts,
579 methodologies, prediction and applications–a review. European Journal of Soil Science
580 2009; 60: 590-612.
581 Directive E. Commission Directive 2003/100/EC of 31 October 2003 amending Annex I of
582 Directive 2002/32/EC of the European Parliament and of the Council on undesirable
583 substances in animal feed. Off. J. Eur. Union 2003; 50.
584 Eller F, Brix H. Influence of low calcium availability on cadmium uptake and translocation in a
585 fast-growing shrub and a metal-accumulating herb. AoB Plants 2016; 8.
586 Frick HM, Tardif S, Kandeler E, Holm PH, Brandt KK. Assessment of biochar and zero-valent iron
587 for in-situ remediation of chromated copper arsenate contaminated soil. STOTEN (submitted)
588 Frick HM. Remediation of chromated copper arsenate (CCA) contaminated sites with biochar and
589 zero-valent iron. Faculty of Science. Master's thesis. University of Copenhagen, 2016.
590 Gee GW, Bauder JW. Particle-size analysis. Methods of soil analysis: Part 1—Physical and
591 mineralogical methods 1986: 383-411.
592 Gezer ED, Cooper PA. Effects of wood species and retention levels on removal of copper,
593 chromium, and arsenic from CCA-treated wood using sodium hypochlorite. Journal of
594 forestry research 2016; 27: 433-442.
595 Giller KE, Witter E, McGrath SP. Heavy metals and soil microbes. Soil Biology and Biochemistry
596 2009; 41: 2031-2037.
597 Gräfe M, Tappero RV, Marcus MA, Sparks DL. Arsenic speciation in multiple metal environments:
598 II. Micro-spectroscopic investigation of a CCA contaminated soil. Journal of Colloid and
599 Interface Science 2008; 321: 1-20.
600 Hingston J, Collins C, Murphy R, Lester J. Leaching of chromated copper arsenate wood
601 preservatives: a review. Environmental Pollution 2001; 111: 53-66.
602 Hopp L, Nico PS, Marcus MA, Peiffer S. Arsenic and chromium partitioning in a podzolic soil
603 contaminated by chromated copper arsenate. Environmental science & technology 2008; 42:
604 6481-6486.
605 Hopp L, Peiffer S, Durner W. Spatial variability of arsenic and chromium in the soil water at a
606 former wood preserving site. Journal of contaminant hydrology 2006; 85: 159-178.
607 Humphrey DG. The chemistry of chromated copper arsenate wood preservatives. Reviews in
608 inorganic chemistry 2002; 22: 1-40.

609 Kabata-Pendias A. Trace elements in soils and plants: CRC press, 2010.
610 Legendre P, Anderson MJ. Distance□based redundancy analysis: testing multispecies responses in
611 multifactorial ecological experiments. Ecological monographs 1999; 69: 1-24.
612 Lin Z, Puls R. Adsorption, desorption and oxidation of arsenic affected by clay minerals and aging
613 process. Environmental Geology 2000; 39: 753-759.
614 Loeppert RH, Suarez DL. Carbonate and gypsum. 1996.
615 Lu A, Zhang S, Shan X-q. Time effect on the fractionation of heavy metals in soils. Geoderma
616 2005; 125: 225-234.
617 Maderova L, Watson M, Paton G. . Soil Biology and Biochemistry 2011; 43: 1162-1168.
618 Maechler M, Rousseeuw P, Struyf A, Hubert M, Hornik K. Cluster: cluster analysis basics and
619 extensions. R package version 2012; 1: 56.
620 Manning BA, Goldberg S. Modeling competitive adsorption of arsenate with phosphate and
621 molybdate on oxide minerals. Soil Science Society of America Journal 1996; 60: 121-131.
622 Martınez C, Motto H. Solubility of lead, zinc and copper added to mineral soils. Environmental
623 Pollution 2000; 107: 153-158.
624 Masscheleyn PH, Delaune RD, Patrick Jr WH. Effect of redox potential and pH on arsenic
625 speciation and solubility in a contaminated soil. Environmental science & technology 1991;
626 25: 1414-1419.
627 Namiesnik J, Rabajczyk A. Speciation analysis of chromium in environmental samples. Critical
628 reviews in environmental science and technology 2012; 42: 327-377.
629 Nguyen MTH, Postma D, Trang PTK, Jessen S, Viet PH, Larsen F. Adsorption and desorption of
630 arsenic to aquifer sediment on the Red River floodplain at Nam Du, Vietnam. Geochimica et
631 cosmochimica acta 2014; 142: 587-600.
632 Nielsen SS, Jakobsen R, Kjeldsen P. Lokalitet nr. 219-3 Collstrupgrunden: Udredning vedr.
633 forureningssituationen på og omkring grunden 1977–2009 (In Danish). 2010.
634 Nielsen SS, Jakobsen R, Kjeldsen P. Stabilization of arsenic and chromium polluted soils using
635 water treatment residues. 2013.
636 Nielsen SS, Kjeldsen P, Hansen HCB, Jakobsen R. Transformation of natural ferrihydrite aged in
637 situ in As, Cr and Cu contaminated soil studied by reduction kinetics. Applied geochemistry
638 2014; 51: 293-302.
639 Nielsen SS, Kjeldsen P, Jakobsen R. Full scale amendment of a contaminated wood impregnation
640 site with iron water treatment residues. Frontiers of Environmental Science & Engineering
641 2016; 10: 3.
642 Noll MR. Trace elements in terrestrial environments: biogeochemistry, bioavailability, and risks of
643 metals. Journal of Environmental Quality 2003; 32: 374.
644 Nunes I, Jacquiod S, Brejnrod A, Holm PE, Johansen A, Brandt KK, et al. Coping with copper:
645 legacy effect of copper on potential activity of soil bacteria following a century of exposure.
646 FEMS microbiology ecology 2016; 92: fiw175.
647 Nybroe O, Brandt KK, Ibrahim YM, Tom□Petersen A, Holm PE. Differential bioavailability of
648 copper complexes to bioluminescent Pseudomonas fluorescens reporter strains.
649 Environmental toxicology and chemistry 2008; 27: 2246-2252.
650 Oksanen J, Blanchet FG, Kindt R, Legendre P, Minchin PR, O'hara R, et al. Package 'vegan'.
651 Community ecology package, version 2013; 2.
652 Ore S, Mertens J, Brandt KK, Smolders E. Copper toxicity to bioluminescent Nitrosomonas
653 europaea in soil is explained by the free metal ion activity in pore water. Environmental
654 science & technology 2010; 44: 9201-9206.
655 Peijnenburg WJ, Zablotskaja M, Vijver MG. Monitoring metals in terrestrial environments within a
656 bioavailability framework and a focus on soil extraction. Ecotoxicology and environmental
657 safety 2007; 67: 163-179.
658 Rowell D. SoilScience: methods & applications.,(Longman Scientific & Technical: Harlow, UK).
659 Soil science: Methods and applications. Longman Scientific and Technical, Harlow, UK.
660 1994: -.

661 Samfundsteknik. Pollution Investigation of the Former Impregnation Facility, Stenholtsvang – Fase
662 1 (in Danish). County of Frederiksborg, Denmark (1989) 1989a.
663 Samfundsteknik. Stenholtvang, Pollution Investigation – Fase 2 (In Danish). County of
664 Frederiksborg, Denmark (1989) 1989b.
665 Wickham H. Reshaping data with the reshape package. Journal of Statistical Software 2007; 21: 1-
666 20.
667 Wickham H. ggplot2: elegant graphics for data analysis. J Stat Softw 2010; 35: 65-88.
668 Wragg J, Cave M. Assessment of a geochemical extraction procedure to determine the solid phase
669 fractionation and bioaccessibility of potentially harmful elements in soils: A case study
670 using the NIST 2710 reference soil. Analytica Chimica Acta 2012; 722: 43-54.
671 Wragg J, Cave M, Gregory S. The solid phase distribution and bioaccessibility of arsenic,
672 chromium, and nickel in natural ironstone soils in the UK. Applied and Environmental Soil
673 Science 2014; 2014.
674 Yang J-K, Barnett MO, Jardine PM, Basta NT, Casteel SW. Adsorption, sequestration, and
675 bioaccessibility of As (V) in soils. Environmental Science & Technology 2002; 36: 4562-
676 4569.
677 Young SD. Chemistry of heavy metals and metalloids in soils. Heavy metals in soils. Springer,
678 2013, pp. 51-95.
679 Yu S, He Z, Huang C, Chen G, Calvert D. Copper fractionation and extractability in two
680 contaminated variable charge soils. Geoderma 2004; 123: 163-175.
681 Zachara JM, Kukkadapu RK, Fredrickson JK, Gorby YA, Smith SC. Biomineralization of poorly
682 crystalline Fe (III) oxides by dissimilatory metal reducing bacteria (DMRB).
683 Geomicrobiology Journal 2002; 19: 179-207.

684

Figures and Tables

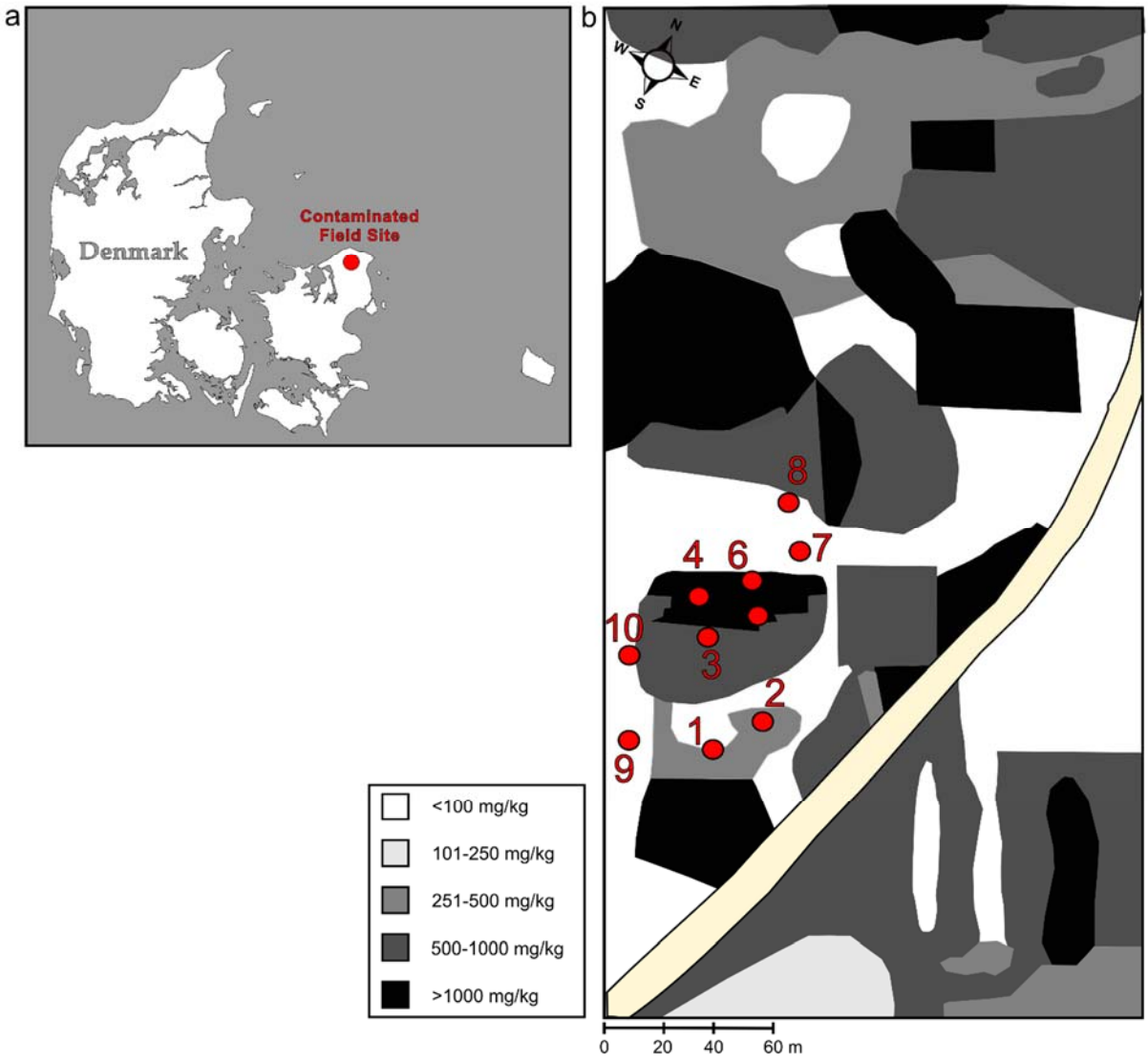

Figure 1: (a) Map of Denmark and location of contaminated field site and (b) field site with cumulative total Cr, Cu and As concentrations measured in 1990 by SAMFUNDSTEKNIK during phase 2 risk assessment (Samfundsteknik, 1989b) with designated 10 sampling locations (1-10).

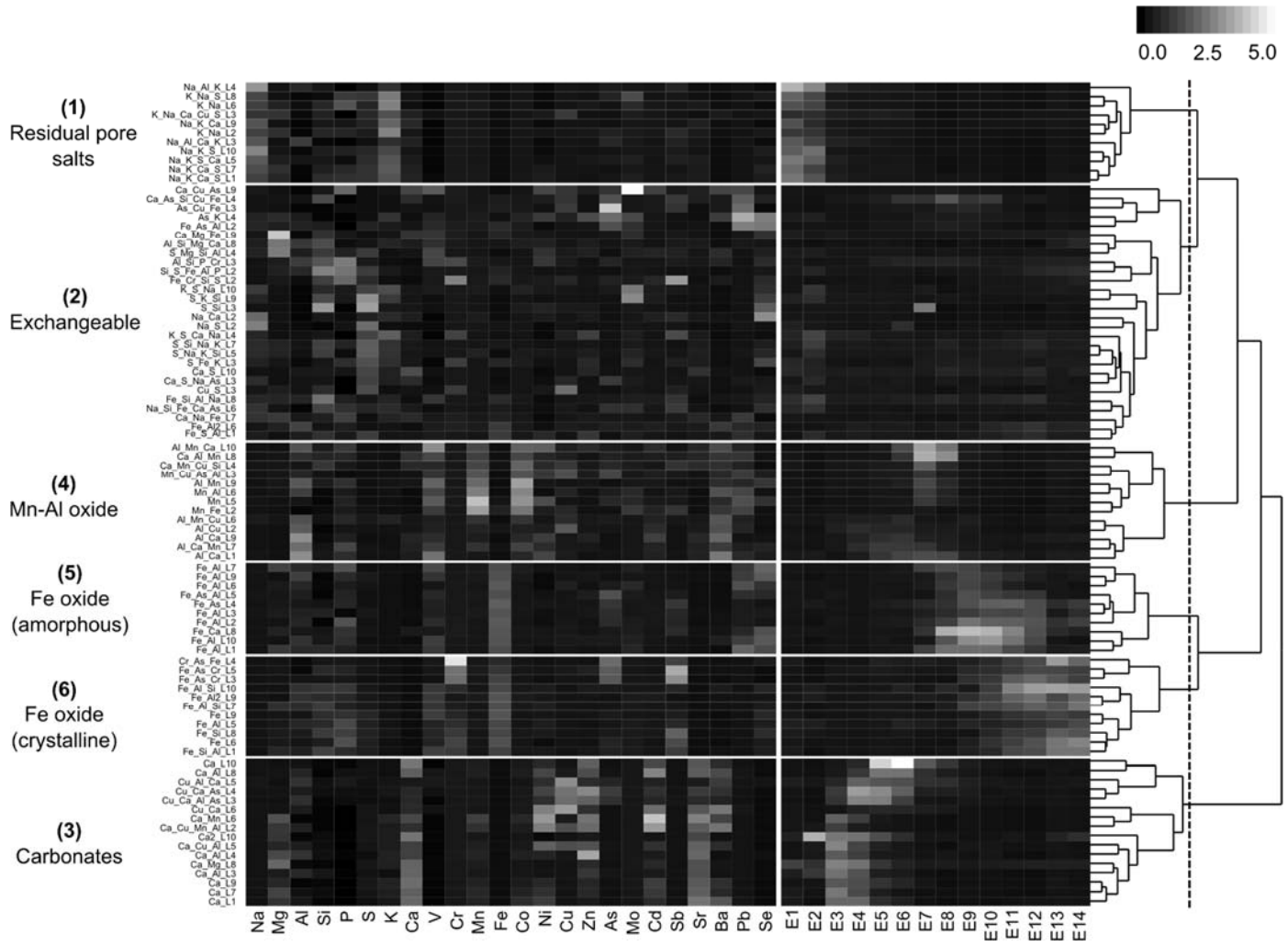

Figure 2: Heatmap and hierarchal clustering of components identified by self-modelling mixture resolution (SMMR) algorithm for 10 sampling locations. The heatmap color gradient represents the mean-centered concentrations of elements and the extraction profiles (E1-E14) reported as total extracted solids (μg g^{-1}) of the individual components, where black is low and white represents high concentrations. Each row represents a component identified by the SMMR algorithm with the name indicating the origin of the sampling location and the major elemental composition (≥10%). The stipple line on the ward cluster tree is where the cut-off was made to inform the geochemical assignment of common soil solid phases, listed in decreasing extractability; 1) Residual pore salts, 2) Exchangeable, 3) Carbonates (tentative designation), 4) Mn-Al oxide, 5) Fe oxide (amorphous) and 6) Fe oxide (crystalline).

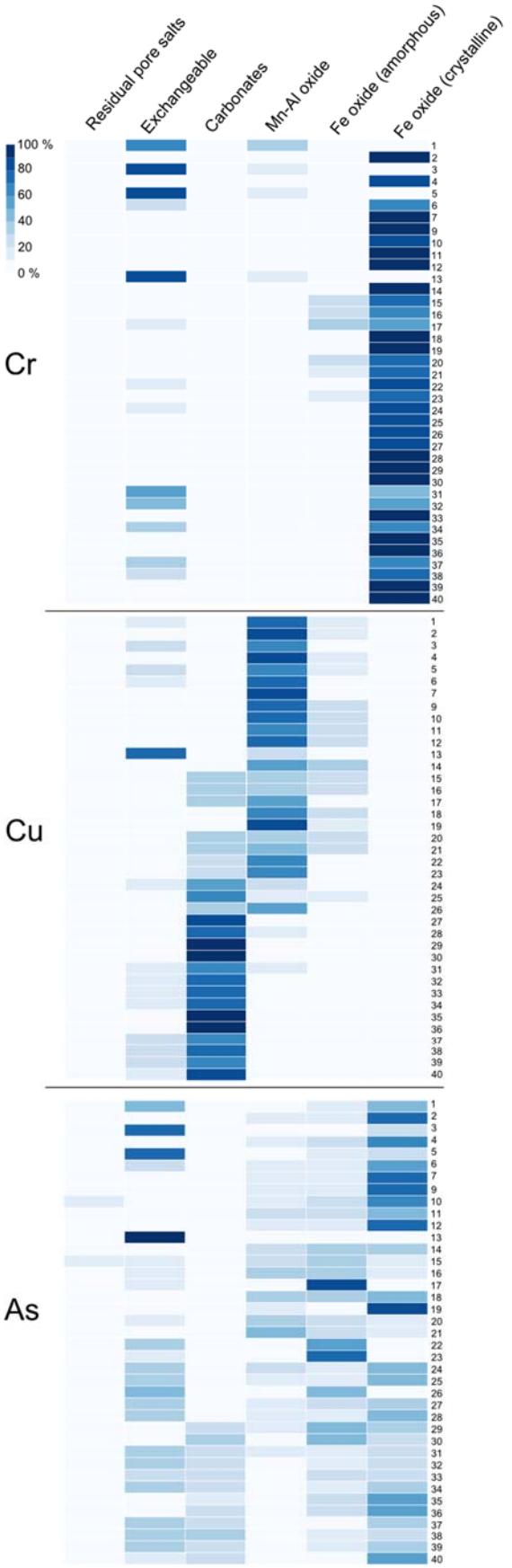

Figure 3: Distribution (%) of Cr, Cu and As in different geochemical soil phases as compared to total extracted using CISED, in decreasing ease of extractability from the soil samples, along contamination gradient in Fredensborg, Denmark.

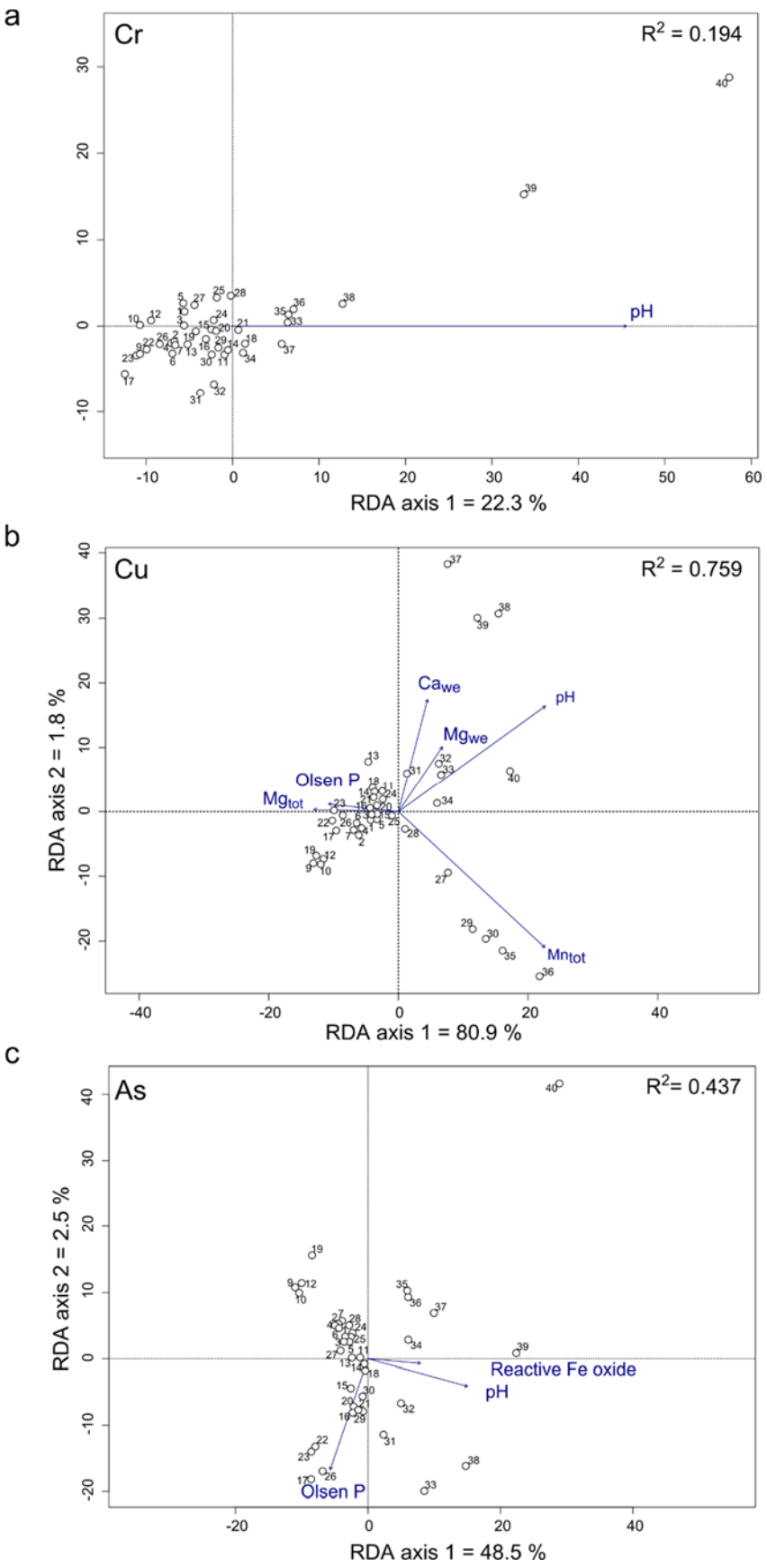

Figure 4: The effect of significant (p≥0.05) physico-chemical factors on the solid phase distribution measured using CISED of (a) Cr (one-dimensional), (b) Cu and (c) As shown using constrained partial redundancy analysis, while controlling for the effect of autospatial correlation of sample.

764 **Table 1:** Selected physico-chemical properties of the top 10 cm of soil sampled (*n*=40) along the contamination gradient in Fredensborg, Denmark

Sample[a]	Sampling Location[b]	Clay[c]	Silt[c]	Sand[c]	Texture[c]	pH	C	N	Olsen P	Reactive Fe oxides	Cu_{Bio}[d]	As_{tot}[d]	Ca_{we}[d]	Cr_{tot}[d]	Cu_{tot}[d]	Mg_{tot}[d]	Mn_{tot}[d]	P_{tot}[d]	As_{we}[d]	Ca_{we}[d]	Cr_{we}[d]	Cu_{we}[d]	Mg_{we}[d]	Mn_{we}[d]
		%			USDA		%		mg g-1		µg g-1													
1	9	6	13	81	Loamy sand	4.56	2.93	0.18	20.2	5.97	0.06	32.5	2441	28.9	17.2	1565	521	460	0.17	8.04	0.04	0.11	1.05	0.39
2	7	4.4	13.6	82	Loamy sand	5.27	2.69	0.14	32.1	1.48	0.40	39.8	2538	30.4	32.3	1672	457	403	0.40	18.8	0.13	0.56	4.78	2.45
3	9	6	13	81	Loamy sand	5.01	2.92	0.17	19.4	4.98	0.05	46.1	2524	33.4	24.0	1648	492	443	0.22	7.12	0.02	0.11	0.77	0.20
4	7	4.4	13.6	82	Loamy sand	5.26	2.5	0.13	27.3	1.98	0.25	36.7	2480	26.1	42.4	1622	445	399	0.24	11.2	0.06	0.38	2.27	0.70
5	9	6	13	81	Loamy sand	4.29	3.21	0.19	24.0	2.19	0.10	61.5	1997	30.4	22.9	1334	441	403	0.37	7.35	0.03	0.18	0.97	0.40
6	7	4.4	13.6	82	Loamy sand	5.64	3.83	0.21	27.9	2.2	0.32	48.0	2759	47.1	52.2	1455	447	394	0.67	26.0	0.17	0.70	4.70	1.38
7	7	4.4	13.6	82	Loamy sand	5.29	5.91	0.27	41.2	1.87	0.34	54.0	3137	59.0	52.8	1747	496	492	0.61	15.7	0.13	0.48	2.91	1.02
8	10	4	13	83	Loamy sand	6.42	11.6	0.6	29.6	2.95	0.14	109	3307	67.2	75.3	1550	463	538	2.19	36.1	0.04	0.38	2.02	0.09
9	1	6.4	8	85.6	Sand	4.53	9.55	0.56	14.7	1.73	0.19	109	2869	94.4	70.0	1535	276	455	1.22	13.7	0.15	0.60	1.73	0.47
10	1	6.4	8	85.6	Sand	3.53	12.6	0.69	18.2	1.93	0.21	113	3408	110	69.6	1601	304	486	1.79	17.8	0.21	0.48	2.55	1.03
11	10	4	13	83	Loamy sand	6.73	7.89	0.41	22.1	1.61	0.04	169	4596	94.0	93.9	1627	543	539	2.02	30.6	0.03	0.23	2.72	0.13
12	1	6.4	8	85.6	Sand	3.64	9.15	0.51	19.4	2.02	0.38	143	2847	128	94.6	1520	282	459	1.62	25.8	0.27	0.96	3.08	1.90
13	9	6	13	81	Loamy sand	5.62	4.24	0.25	31.0	1.89	0.09	178	4584	107	137	1584	533	633	0.54	6.31	0.03	0.14	0.98	0.24
14	10	4	13	83	Loamy sand	6.78	12.9	0.62	37.3	1.78	0.05	175	7414	142	122	1591	616	671	1.97	45.6	0.04	0.24	4.96	0.10
15	8	4	9	87	Sand	5.55	10.3	0.56	59.4	1.99	0.18	213	4775	154	158	1707	449	557	5.44	27.4	0.29	0.79	6.72	0.66
16	8	4	9	87	Sand	5.78	11.3	0.58	42.2	2.16	0.62	288	5021	128	149	1787	508	562	4.98	22.7	0.15	0.65	4.95	0.25
17	2	5.6	5.4	89	Sand	5.08	2.63	0.17	73.4	4.52	1.93	251	1399	74.2	289	872	225	516	4.80	5.11	0.13	1.69	1.34	0.70
18	10	4	13	83	Loamy sand	6.75	10.3	0.51	35.0	2.57	0.09	294	6797	161	203	1839	678	712	2.49	41.0	0.04	0.35	2.70	0.09
19	1	6.4	8	85.6	Sand	4.73	11	0.58	20.4	2.15	0.59	284	3637	244	134	1594	339	463	2.94	26.8	0.44	1.15	3.17	1.25
20	8	4	9	87	Sand	5.67	10	0.55	39.0	1.95	0.28	313	5294	169	188	1924	687	699	5.24	24.3	0.15	0.68	5.01	0.31
21	8	4	9	87	Sand	5.96	7.1	0.39	45.3	2.15	0.71	228	6096	213	251	1951	747	645	6.21	23.9	0.22	0.86	5.13	0.32
22	2	5.6	5.4	89	Sand	4.45	2.85	0.17	68.6	2.25	0.87	334	1144	216	281	755	230	384	7.63	3.42	0.23	1.51	1.00	0.69
23	2	5.6	5.4	89	Sand	4.51	2.56	0.16	59.5	1.91	1.53	221	1112	147	493	725	258	428	3.18	3.54	0.14	2.09	0.66	0.46
24	6	5.6	9.4	85	Sand	5.07	5.43	0.29	47.3	2.2	1.00	308	1564	267	371	898	623	576	5.33	4.71	0.29	1.47	1.21	0.51
25	6	5.6	9.4	85	Sand	4.38	7.93	0.41	40.8	2.1	0.72	386	1519	440	468	919	536	567	8.43	5.02	0.72	1.57	1.64	0.93
26	2	5.6	5.4	89	Sand	4.67	2.96	0.18	65.9	1.96	1.22	397	1169	372	561	721	434	438	3.87	4.02	0.21	1.59	0.94	0.60
27	6	5.6	9.4	85	Sand	4.2	17.4	0.83	22.2	2.17	3.52	203	1749	187	1129	692	484	445	7.51	11.2	0.35	5.99	2.36	0.90

28	6	5.6	9.4	85	Sand	4.59	7.03	0.38	34.5	2.44	1.92	404	1925	568	674	864	683	582	5.84	10.9	0.78	2.98	2.71	1.06
29	5	2.4	6.6	91	Sand	6	2.57	0.17	26.3	2.4	1.03	459	1899	283	965	1095	1142	474	4.79	6.53	0.09	1.64	1.03	0.15
30	5	2.4	6.6	91	Sand	6.21	1.88	0.14	26.1	2.67	1.28	470	1818	239	1298	978	834	428	6.52	12.1	0.13	2.69	2.16	0.17
31	3	4.4	4.6	91	Sand	6.83	1.6	0.1	29.3	1.94	0.23	857	3285	336	879	1106	536	356	4.15	36.9	0.11	0.67	2.36	0.08
32	3	4.4	4.6	91	Sand	6.65	1.66	0.09	37.5	2.35	1.31	1088	3692	399	1097	1079	461	361	4.59	50.8	0.09	0.84	2.56	0.10
33	4	4.4	10.6	85	Loamy sand	6.35	2.4	0.12	27.4	3.87	1.01	1139	2400	434	1158	1124	385	319	18.4	15.7	0.29	3.66	4.05	0.86
34	3	4.4	4.6	91	Sand	6.21	1.47	0.09	26.6	2.43	1.34	1097	2509	555	1168	1144	343	363	7.65	37.5	0.24	2.02	3.02	0.16
35	5	2.4	6.6	91	Sand	6.23	1.76	0.11	24.8	1.48	0.76	973	2394	526	1462	1083	869	344	9.09	21.7	0.11	1.62	4.12	0.82
36	5	2.4	6.6	91	Sand	6.08	1.79	0.11	30.4	2.37	0.51	859	2442	456	1935	1172	1174	372	6.45	12.8	0.09	1.60	2.33	0.29
37	3	4.4	4.6	91	Sand	6.54	1.54	0.1	25.1	3.27	1.52	1357	2633	641	1785	977	397	350	7.63	47.3	0.24	2.05	2.70	0.13
38	4	4.4	10.6	85	Loamy sand	6.42	1.7	0.09	29.5	3.6	1.15	1795	4030	263	2205	1239	459	341	11.8	20.3	0.52	4.80	4.83	0.38
39	4	4.4	10.6	85	Loamy sand	6.27	2.16	0.11	23.9	3.49	0.60	2028	3867	1171	1844	1221	445	378	9.51	19.7	0.15	1.69	4.19	0.13
40	4	4.4	10.6	85	Loamy sand	6.26	3.08	0.11	25.3	3.99	0.58	2839	3038	1819	1630	1201	469	341	10.8	12.9	0.31	2.31	3.80	0.37

765

766 [a] Samples were named 1-40 by total cumulative concentrations of Cr, Cu and As in ascending order

767 [b] Four samples were obtained from each sampling location (see Figure 1 for details)

768 [c] Clay, silt, sand and texture classification were performed on composite sample at each sampling location

769 [d] Cu_{bio}=bioavailable Cu as determined by whole-cell bacterial bioreporter assay, tot=total extracted by aqua regia digestion and we= water-extractable
770 concentrations

771

772

773

774

775

776

777

778 **Table 2:** Common soil solid phases identified by CISED sequential extraction along the contamination gradient in Fredensborg, Denmark

779

Soil Phase	Major element composition	Minor element composition	Extraction profile example	References[a]
Residual pore-salts	Al, Ca, Na, K, and S	Si	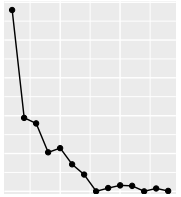	(Cave et al., 2004; Rowell, 1994)
Exchangeable	K, Na, Mg, S, Si and K	Sb, Se and P	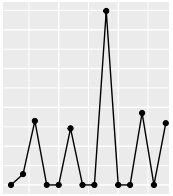	(Rowell, 1994)
Carbonates (tentative designation)	Ca and Mg	Al, Ba, Cd, Cu, Sr and Zn	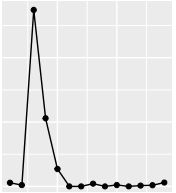	(Loeppert and Suarez, 1996)
	Ca	Al, Ba, Cd, Cu, Sr and Zn	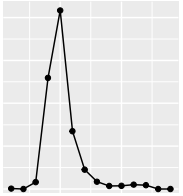	(Loeppert and Suarez, 1996)
Mn-Al oxides	Mn and Al		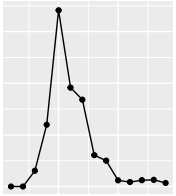	(Manning and Goldberg, 1996; Young, 2013)

Fe oxide (amorphous)	Fe and Al	Pb, Se and V	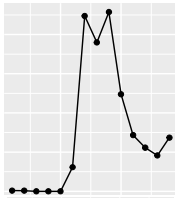	(Cave et al., 2004; Cave and Wragg, 1997; Cornell and Schindler, 1987)
Fe oxide (crystalline)	Fe	Al and Si	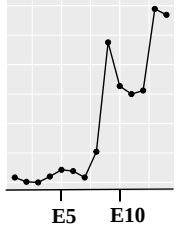	(Cave et al., 2004; Cave and Wragg, 1997; Cornell and Schwertmann, 2003)

780

781 [a]References which informed the grouping into common soil phases